Copyright Assignment

This form is intended for original material submitted to the CSCE for publication of papers in the Conference Proceedings. This form must accompany any such material in order to be published by the CSCE.

THE EFFECT OF CIRCUMFERENTIAL FLAWS ON THE STRAIN CAPACITY OF PRESSURIZED X52 PIPELINES

Complete list of authors:
Diana Abdulhameed, University of Alberta, Edmonton, AB, Canada.
Celal Cakrioglu, University of Alberta, Edmonton, AB, Canada.
Millan Sen, Enbridge Pipelines, Edmonton, Alberta, Canada.
John Nychka, Univeristy of Alberta, Edmonton, AB, Canada.
J.J. Cheng, Univeristy of Alberta, Edmonton, AB, Canada.
Samer Adeeb, Univeristy of Alberta, Edmonton, AB, Canada.

Conference publication title:
Proceedings of the Annual Conference and General Meeting of the CSCE - 2015.

Signature of Author/Authorized Agent for Joint authors:	Date:
Diana Abdulhameed	March 8th, 2015.

NOTE: Please upload your signed copy to the event management website.

THE EFFECT OF CIRCUMFERENTIAL FLAWS ON THE STRAIN CAPACITY OF PRESSURIZED X52 PIPELINES

Diana Abdulhameed, University of Alberta, Edmonton, AB, Canada.
Celal Cakrioglu, University of Alberta, Edmonton, AB, Canada.
Millan Sen, Enbridge Pipelines, Edmonton, Alberta, Canada.
John Nychka, Univeristy of Alberta, Edmonton, AB, Canada.
J.J. Cheng, Univeristy of Alberta, Edmonton, AB, Canada.
Samer Adeeb, Univeristy of Alberta, Edmonton, AB, Canada.

Abstract:

Tensile strain capacity (TSC) of pipelines with girth weld flaws have been traditionally measured experimentally using wide plate tests. However, Numerical analysis in recent studies showed that the TSC are affected by the level of internal pressure inside the pipeline, Y.Wang (2008). Most of the past studies focused on the effect of circumferential flaws on the TSC for pipelines of steel grade X65 or higher. The current Oil and Gas Pipeline System Code CSA Z662-11 provide equations to predict the critical TSC as a function of geometry and material properties of the pipelines. These equations were based on extensive studies on pipes having grades X65 or higher without considering the effect of internal pressure which makes it beneficial to be investigated. In this study, eight full-scale experimental tests of NPS 12" pipes with 6.91 mm wall thickness and grade X52 were conducted in order to investigate the effect of circumferential flaws close to a girth weld on the TSC for vintage pipelines subjected to eccentric tensile forces and internal pressure. A digital image correlation system and biaxial strain gauges were used to obtain the tensile strain along the pipe length during the test. Post-failure macro-fractography analysis was used to confirm the original size of the machined flaw and to identify areas of plastic deformation and brittle/ductile fracture surfaces. From the experimental and numerical results, the effect of internal pressure and flaw size on the TSC was investigated. The CMOD at failure for different pipes were compared.

1 INTRODUCTION

In arctic and seismically active regions, pipelines may experience high longitudinal plastic strains that cause high longitudinal deformations. The high strain could be resulted from large ground movements such as seismic activity, slope instability or temperature variations in addition to internal pressure. Fabrication flaws that exist in girth welds are one of the major reasons leading to failure of a pipeline due to high tensile longitudinal strains. In order to avoid failures in the pipeline due to high tensile strains, the dimensions of the inevitable fabrication flaws in girth welds need to be restricted within acceptable limits. The lack of knowledge about the effects of flaw sizes and internal pressure on the structural behaviour of a pipeline can lead to violating the design limit states. This violation may cause loss of life and property, damage to the environment, and derangement of pipeline operations. Therefore, there is a direct impact on the safety and integrity of pipeline systems by developing the tensile strain design models. In order to understand the structural behaviour of a pipeline in the presence of fabrication flaws and internal pressure, it is necessary to conduct full-scale tests of the pipe for different crack sizes and internal pressure levels.

In previous studies, the frequently used technique has been the curved wide plate (CWP) tests to evaluate the tensile stresses and strains of pipelines with a girth weld without considering the effect of internal pressure on pipelines behaviour. The current CSA Z662 [1] adopts tensile strain equations published in Annex C that were validated against CWP test data based on extensive research of Wang et al [2] where the internal pressure effect was not considered. Recently, Some studies based on numerical analysis have proven that internal pressure will lead to a reduction in the tensile strain capacity of a pipeline [3]. Ostby and Hellesvik, 2007 [4] conducted full-scale tests and compared the data with numerical analysis results. Both results showed good agreement and indicated the effect of internal pressure on the tensile strain capacity of pipes. Many industrial companies in North America are investigating the tensile strain capacity of girth weld pipelines in harsh arctic or seismically active regions. Currently, two main projects are investigating the strain-based design of pipelines; a research project supported by PRCI [5] published equations to evaluate the tensile strain capacity of pipelines beyond yield strain. This study involved fundamental fracture mechanics, small-scale material characterization tests, and full-scale tests of pipes. Another ongoing research is conducted by ExxonMobil [6 - 8] based on extensive numerical analysis and full-scale pipe tests to derive a parametric equation for the tensile strain capacity. The investigation is CTOD (Crack tip opening displacement) based and a multi-tier level of engineering critical assessment was proposed. Currently, two levels were published. Level 1 being the more simplified equation and level 2 is the complicated equation involving FEA analysis. These previous studies were conducted on pipes with grade X65 or higher, therefore, it is beneficial to analyse the variation of tensile strain capacity for vintage pipelines with grade X52 at different internal pressure levels.

The scope of this paper covers the effect of surface type girth weld flaws on the tensile strain capacity of X52 vintage pipes under internal pressure. In order to investigate this effect, eight full-scale tests were investigated under different levels of internal pressure and a flaw was machined near a girth weld with different sizes. The experimental results concluded that the internal pressure causes a significant reduction in the tensile strain capacity of the pipeline. In addition, the flaw depth was found to have the greatest effect on the TSC when compared to the effect of flaw length. Moreover, the test results showed that the level of internal pressure has no effect on the final CMOD at failure for two tests with consistent flaw size. The experimental setup and the results of the eight full-scale tests are presented in this paper.

2 METHODOLOGY

2.1 Full-scale Test Setup

Full-scale tests were conducted on vintage pipes to investigate the effect of internal pressure on the tensile strain capacity of pipelines with flaws near the girth weld. The tested pipes were NPS 12” of grade X52 having an outer diameter of 12.75” (324mm) and nominal wall thickness 0.273” (6.95 mm) being cut out of the Norman Wells pipelines. Small-scale tension coupon tests were conducted to determine the tensile properties of the pipe base metal and girth welds [1]. The X52 pipes had specified minimum yield strength (SMYS) of 359 MPa (52 KSI) and an average yield to tensile (Y/T) ratio equal 0.717. Table (1) presents the test matrix for the eight full-scale pipe experiments, showing the flaw sizes and pipe lengths. The pipe length varied according to the availability of cut out parts from the main pipe. A flaw was introduced close to the girth weld by a machined saw cut. The flaw dimensions had two lengths (50 mm and 150 mm) with a depth of 25% or 50% of the nominal wall thickness (1.3mm and 3.4mm). The pipes were tested in an MTS machine under eccentric tensile displacement in the presence of internal pressure. The eccentricity was introduced to ensure that the circumferential flaw was exhibiting the highest tensile strain throughout the test.

The loading in all tests was applied in two steps. In the first step, the internal pressure that causes 30% and 80% SMYS hoop stress was calculated using the Barlow's formula and was applied by filling the pipe with water through an opening located in the bottom end plate. Another opening at the top end plate was provided to avoid any trapped air in the pipe throughout the filling process and was closed with a ball valve once the pipe is completely filled with water. The level of internal pressure was controlled and monitored with a pressure relief valve connected to the bottom end plate that has a capacity of 12 MPa (1750 PSI). In the second step, the internal pressure was kept constant while the eccentric tensile displacement was applied to the top end plate in increments until the point in time where the water seeps out of the crack, which is defined as the instance of failure.

Table 1: Test Matrix

Test	Pipe Length (mm)	Internal Pressure applied	Flaw depth (mm)	Flaw length (mm)
1	1828.8	80%	1.7	50
2	1828.8	30%	1.7	50
3	1828.8	80%	3.4	50
4	1828.8	30%	3.4	50
5	1219.2	80%	1.7	150
6	1219.2	30%	1.7	150
7	1219.2	80%	3.4	150
8	1219.2	30%	3.4	150

The instrumentation plan was designed to evaluate and record the strains along the pipe length throughout the test. A digital image correlation (DIC) technique was used to obtain the strain variation along the pipe length at the tension side during each experiment. In addition, axially and circumferentially strain gauges were positioned at a quarter of the pipe length away from the cap plate and at 90 degrees intervals of the pipe circumference. The reaction force and displacement during the test were measured and recorded by the MTS. All tests were conducted at room temperature.

For test 1 and 2, The DIC was recording the strain readings on two specific areas. First area had a length of 1.25-OD with the mid-length lying on the crack location. However, the second area had a length of 0.7-OD from the cap plates. For test 3 to 8, the DIC was used to record the strain readings along the full pipe length. Figure (1) shows the paint and speckle pattern used for the DIC technique.

The crack growth during the experiment was observed by developing the crack mouth opening displacement (CMOD) for each test. The displacement of two points lying on each side of the flaw was recorded throughout the test up to failure. The average distance between the two points for all tests had an initial value equal to 10 mm. The digital image correlation (DIC) technique was used to evaluate the displacements for the chosen two points and plot it against the applied MTS load. The distance between the two chosen points were minimized to reduce the pipe strain effect on the CMOD values.

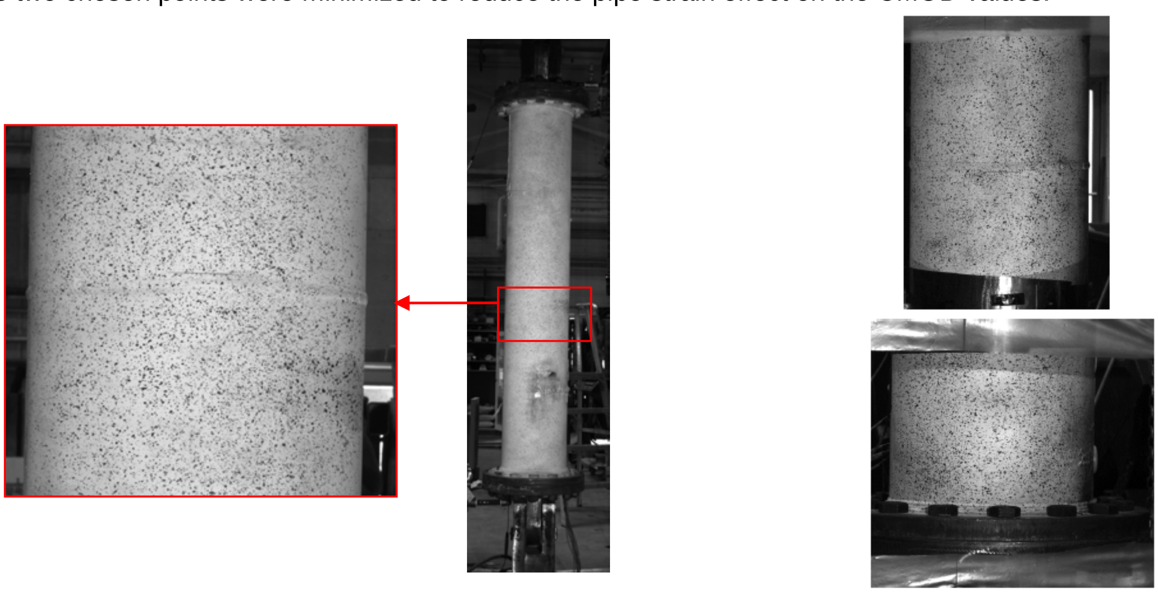

(a) Speckle pattern for Tests 3 to 8 (b) Speckle pattern for Tests 1 and 2

Figure 1: Speckle pattern of DIC system

3 RESULTS AND DISCUSSION

3.1 Full-Scale Test Results

3.1.1 Experimental Strain Results

The remote strain is defined as the strain reading at a quarter of the pipe length from the end plate. This location was decided to be one of the remote strain measurements as it represents the flat part in the strain profile along the pipe length, where the effect of the crack on the TSC is not sensed and the effect of the end connections are not reflected on the TSC values. The remote strain is denoted by $\varepsilon_{0.5L}$. The tensile strains measured by the strain gauges on the tension side of the pipe aligned with the circumferential flaw were used in comparison with the DIC strain readings to validate both measuring instruments. The DIC and strain gauge readings at a quarter of the pipe length from the cap plate were plotted against the applied load up to failure as shown in Figure (2). Tests 1 and 2 were not used in the comparison between the DIC and strain gauges since the DIC covered specific areas not recorded by the strain gauges. For tests 3 to 8, both systems readings (DIC and strain gauges) show that they follow the same profile. When the strain exceeded a certain value, the strain gauges failed and the measurements afterwards were based on the DIC alone. Depending on the DIC calibration accuracy, the DIC readings were equal to the strain gauge reading ± 0.02 %. Figure (2) shows that the strain gauges and DIC results have good agreement with differences less than 7% for all tests except test 4 the difference was 15%.

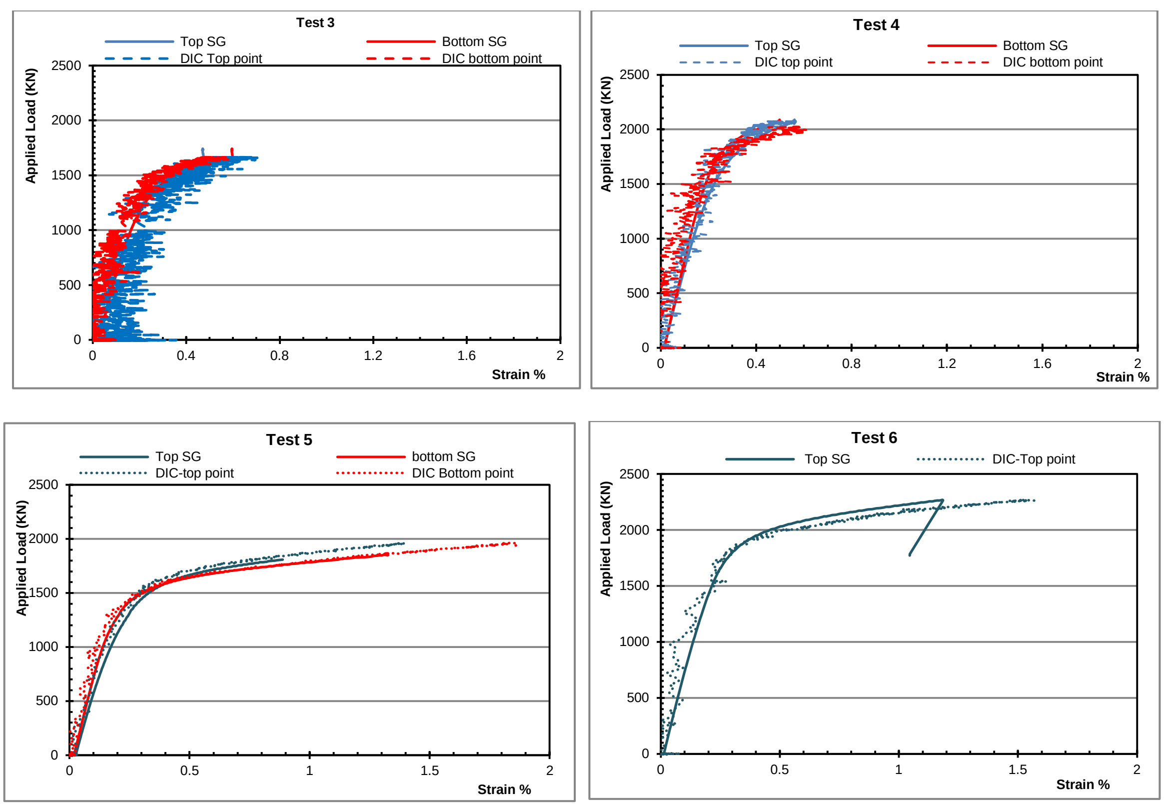

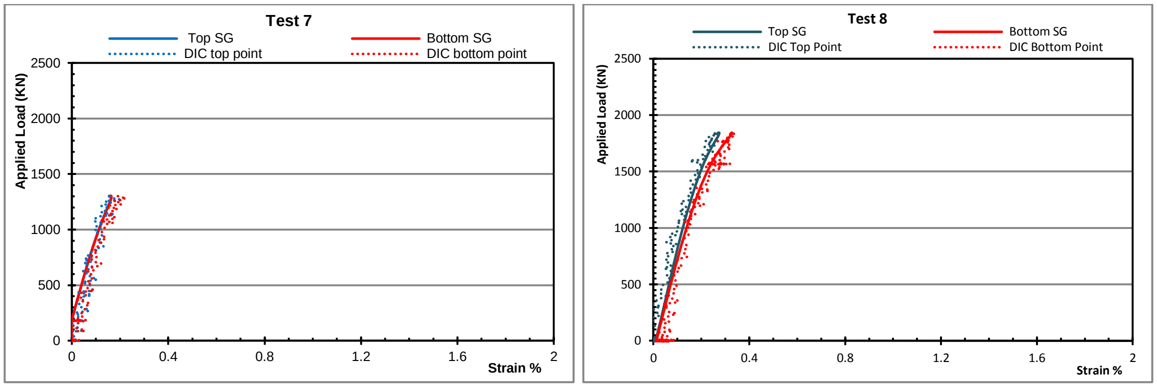

Figure 2: Tensile strain reading from DIC and strain gauges.

3.1.2 Experimental CMOD Results

The CMOD was plotted against the applied load to observe the crack growth during the experiment and up to the point of failure. Two CMOD values are used to compare between two test having the same flaw size, but subjected to different internal pressure levels. First value was the CMOD-failure, which is the CMOD at the failure load by the end of the test. Second value was the CMOD-critical which is at 97% of the failure load. The CMOD-critical is the value of CMOD at a point of time during the test when the applied load is almost constant however the CMOD keeps increasing.

For tests 1 and 2, the CMOD-failure recorded at the end of each test was observed to be 2.15 mm. The CMOD-failure readings for tests 3 and 4 were 2.05 and 2.35 mm respectively. In tests 3 and 4, some cracks formed in the paint layer during loading around the flaw which didn't enable reducing the distance between the two points which accordingly lead to the observed differences (0.3 mm) between the CMOD obtained for test 3 and 4. Tests 5 and 6 had a CMOD-failure of 1.5 mm while tests 7 and 8 had 1.3 mm. The CMOD-critical for tests 1 and 2 was found to be 1.06 mm while for tests 3 and 4 it was 1.013 mm. The CMOD-critical was 0.81 mm for tests 5 and 6, while it was 0.78 mm for tests 7 and 8. This shows that two pipes with consistent flaw and different internal pressure will have the same CMOD when the applied load reaches 97% of the failure load.

The CMOD at failure decreases when the flaw length and flaw depth increase. For two tests with consistent flaw dimensions and different internal pressure, the resulting CMOD was found to be equal as shown in figure (3). This shows that the CMOD is not affected by the change in internal pressure level and accordingly the crack tip opening displacement (CTOD) will not depend on the internal pressure as well. For pipes with high internal pressure (80 % SMYS), the crack will reach to the critical CMOD at lower load and displacement values if compared to pipes with low internal pressure (30% SMYS). In case of tests having short flaws (tests 1, 2, 3 & 4) the load at failure was observed to increase by 24% when the internal pressure was decreased from 80% to 30% SMYS. However, for pipes with long flaws (Tests 5, 6, 7 & 8) the load at failure has an increase of 15% when the internal pressure decreased from 80% to 30% SMYS (Figure (3)). It is observed from the curves that by decreasing the internal pressure level, the applied load required to cause fracture of the flaw will increase and this increase is higher in the case of pipes with a short flaw lengths than pipes with long flaw lengths.

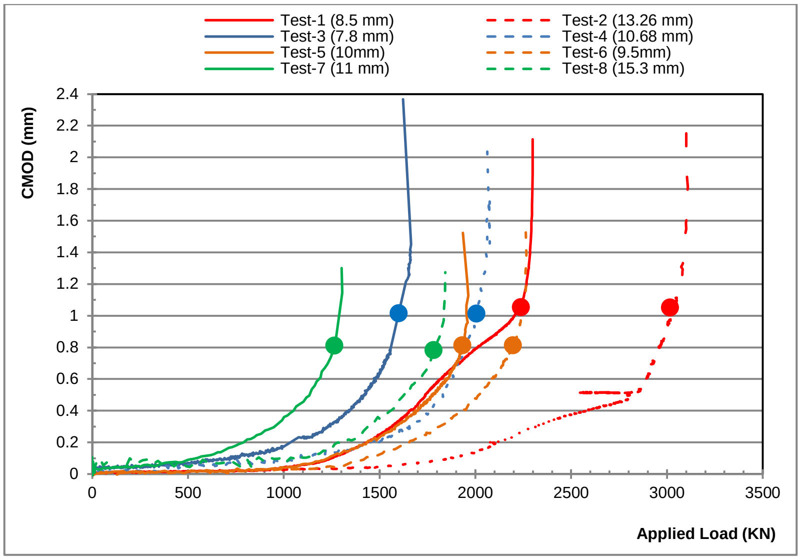

Figure 3: Variation of CMOD (a) Test 1 and Test 2, (b) Test 3 and 4, (c) Test 5 and 6, and(d) Test 7 and 8 (The circles show the location of CMOD-critical for each test)

3.2 Key Parameters Affecting Tensile Strain Capacity

Three main parameters were considered in this study and their effect on the tensile strain capacity of pipelines were investigated: Internal pressure, flaw length and flaw depth. The effect of each parameter is discussed below. The pipe diameter was constant for all tested pipes since its effect on the TSC was found to be weak [9].

3.2.1 Effect of internal pressure

The evaluated remote strain ($\varepsilon_{0.5L}$) was used to compare two pipes with consistent flaw, but different internal pressure levels and show the effect of internal pressure on the TSC. The remote strain ($\varepsilon_{0.5L}$) was plotted against the applied load throughout the test up to failure (Figure (4)). The curves show that the applied load at failure and the axial strain will decrease when the internal pressure increase. When the internal pressure increase, the longitudinal and circumferential tensile stresses on the pipe increase, which cause the crack to fail at lower applied loads.

For tests 1 and 2, the strain gauges on the tension side of the pipe failed before fracture occurred. The curves for tests 1 and 2 give a good indication on how the internal pressure will affect the tensile strains, but these strain gauges were not used to compare the tensile strain at fracture. The DIC technique was used to compare test 1 and 2. The axial strain readings were recorded at length of 0.7-OD (225 mm) and 2.15-OD (700 mm) from the flaw location, then linear interpolation was used for the zone not covered by the DIC. The axial strain at 225 mm was found to be 2.2% for test 1 and 5% for test 2. However, at 700 mm the strain was 4.8% for test 1 and 10% for test 2. This shows that decreasing the internal pressure from 80% SMYS to 30% SMYS will increase the TSC by about 50% between tests 1 and 2. For tests 3 to 8, readings from the DIC and the strain gauges were used to evaluate remote strain ($\varepsilon_{0.5L}$) and both showed good agreement. The evaluated remote strains (Table (2)) show that increasing the internal pressure will result in a decrease in the tensile strain measured. For tests 3 and 4, decreasing the internal pressure from 80% SMYS to 30 % SMYS resulted in increasing the strain by 20%. However, for tests 7 and 8, the increase in strain was found to be 31%. The effect of internal pressure had the highest percentage in the case of tests 1 and 2 when compared with the rest of the tests, since it had the smallest flaw size so it required more energy to cause fracture in the crack. Tests 5 and 6 did not follow the same behaviour of the other test since increasing the internal pressure resulted in a negligible increase in the strain by 5%. There could be many possibilities caused the different pattern that tests 5 and 6 followed. One possibility could be that test 5 had higher material properties from the other pipes or different thickness at the flaw location that increased the pipe resistance to fracture and resulted in higher strains. Another possibility, which is more likely to be the reason for having higher strains in test 5 when compared to test 6, is the existence of multiple notches at the machined flaw that may require more energy to cause crack fracture. A metallurgy test was conducted on all the pipe samples after testing the pipes and the results showed that the pipe in test 5 had a high percentage of multiple notches at the machined flaw that caused an increase in the fracture energy. Accordingly, the higher fracture energy observed in test 5 led to a higher strain that exceeded the strains expected from the case of machined flaw with less notches as the case of test 6.

Table 2: Remote strain evaluated for each test

Test	DIC Remote strain ($\varepsilon_{0.5L}$) %	Strain Gauge ($\varepsilon_{0.5L}$) %
1	2.4	Failed early
2	3.85	Failed early
3	0.51	0.55
4	0.63	0.53
5	1.35	Failed early
6	1.28	Failed early
7	0.20	0.21
8	0.29	0.30

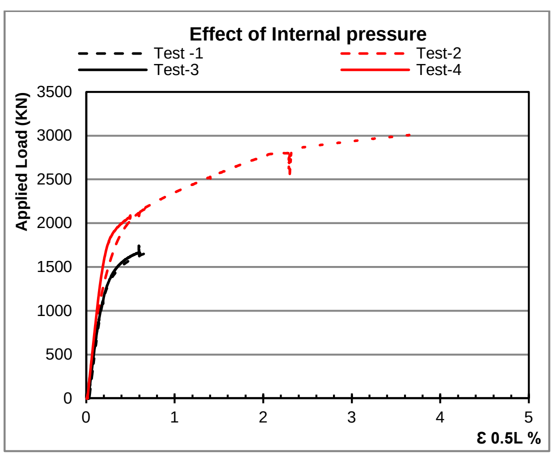

(a)

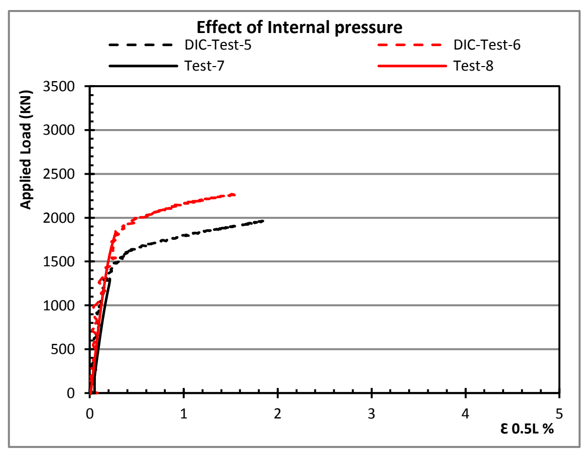

(b)

Figure 4: Variation of internal pressure for tests (a) Test 1, 2, 3 and 4 (b) Test 5, 6, 7 and 8

3.2.2 Effect of flaw size

The applied load is plotted against the remote strain ($\varepsilon_{0.5L}$) up to fracture as shown in figure (5). Each curve shows Four tests that have the same flaw length but different flaw depth and internal pressure level. By comparing two tests having the same internal pressure level will show the effect of flaw depth on the TSC. Figure (5) shows that the TSC decreases drastically by increasing the flaw depth. Increasing the flaw depth from 25% to 50% of the wall thickness will reduce the tensile strain capacity up to 85%. On the other hand, the effect of flaw length on the TSC of the pipe was investigated and shown in Figure (6). Each curve represents four tests having the same flaw depth, but different flaw lengths and internal pressure levels. By comparing two tests subjected to the same level of internal pressure, It was observed that increasing the flaw length resulted in a decrease in the TSC by up to 67%.

The test results showed that the effect of flaw depth was more influential than the effect of flaw length on the TSC. Figure (7) shows the longitudinal strain profile for all eight tests on the tension side of the pipe aligned with the circumferential flaw just before fracture. These curves show that the effect of flaw depth on the tensile strain capacity is more significant than the flaw length for girth weld pipes with circumferential flaw.

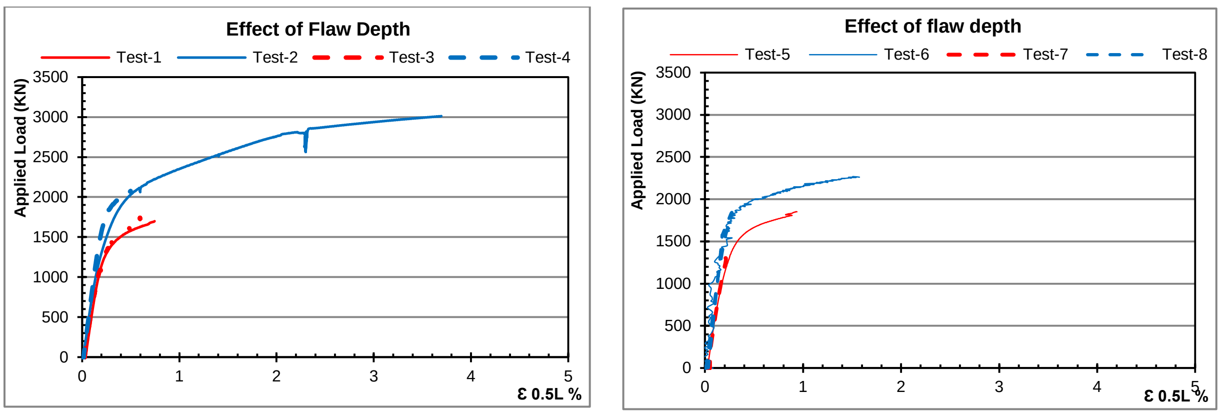

(a) (b)

Figure 5: Load vs. Ɛ0.5L for tests (a) Tests 1, 2, 3 and 4 (b) Tests 5, 6, 7 and 8

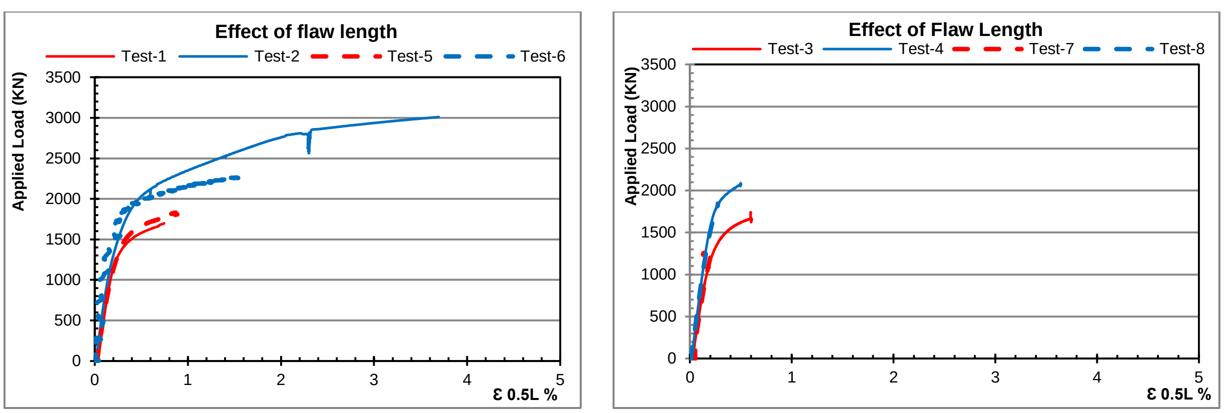

(a) (b)

Figure 6: Load vs. Ɛ0.5L for tests (a) Test 1, 2, 5 and 6 (b) Test 3, 4, 7 and 8

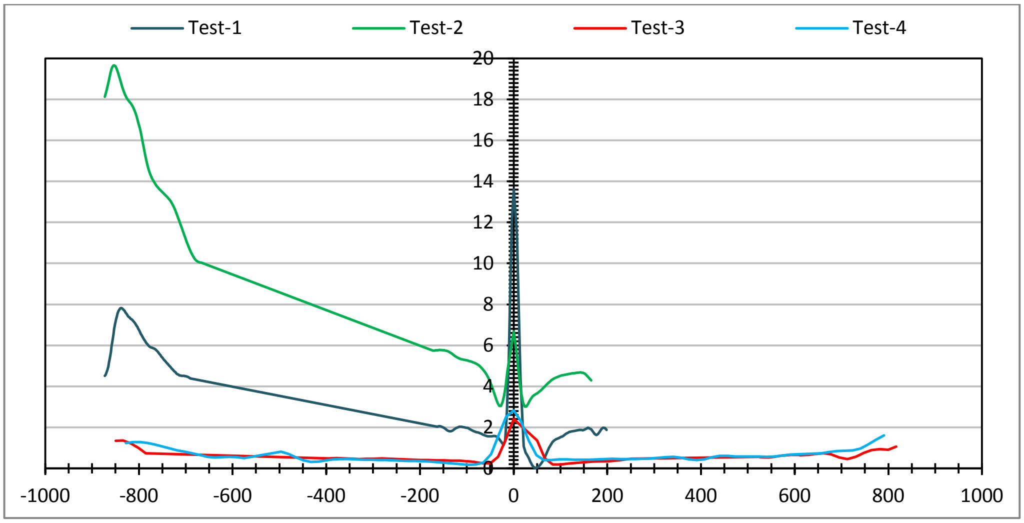

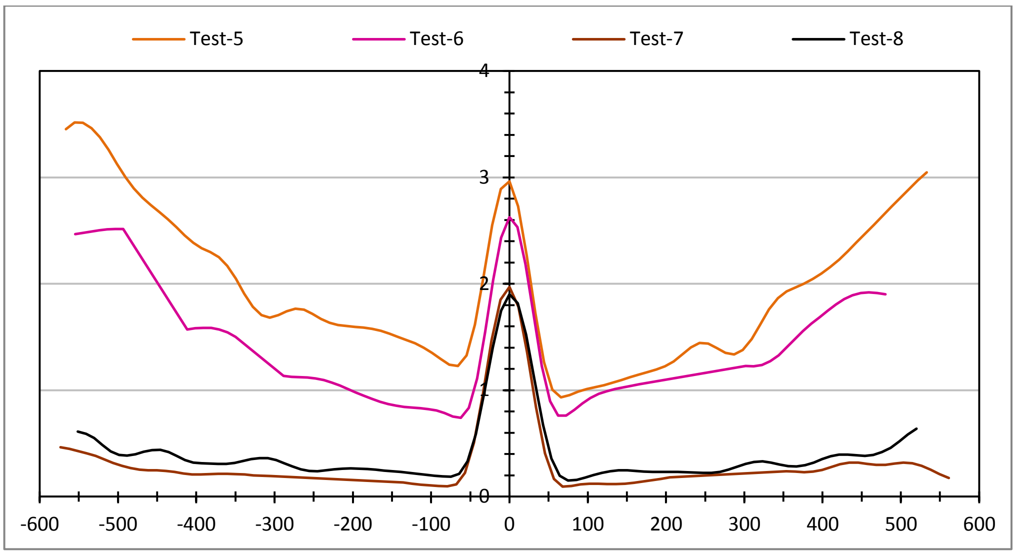

Figure 7: Tensile strain along the pipe length aligned with the flaw

4 CONCLUSION

Most of the past research conducted on girth weld pipelines were investigated using curved wide plate (CWP) tests without considering the effect of internal pressure and these tests were conducted for pipes with grades X65 or higher. The CSA Z662 [1] adopted the equations published in Annex C based on an extensive research of Wang et al [2] based on CWP tests for pipes X65. Recently, some studies considered the effect of internal pressure by conducting full-scale tests on girth weld pipelines with grades X65 and higher and indicated that the internal pressure has a significant effect on the tensile strain capacity [5 - 8].

In this paper, eight full-scale tests with a circumferential flaw close to a girth weld were tested under the effect of internal pressure and eccentric tensile loading in order to evaluate the tensile strain capacity of X52 vintage pipes. The results showed that the tensile strain capacity of welded pipelines is strongly influenced by the level of internal pressure, flaw depth and flaw length. The test results showed that the level of internal pressure could reduce the tensile strain capacity by up to 50% or more depending on the flaw size. On the other hand, the experimental results showed that the CMOD was not affected by the level of internal pressure and was a function in the material properties.

5 ACKNOWLEDGMENT

The authors wish to thank Enbridge for their support in this work and permitting the release of this paper. The pipes used in the experiments provided by Enbidge are very much appreciated. Partial funding for this study was provided by NSERC. The experimental work was conducted by a research group of graduate students under the supervision of Dr. Adeeb at the I.F. Morrison Structural lab, University of Alberta. The authors wish to thank Mr. Greg Miller and Mr. Cameron West at the I.F. Morrison Structural lab, University of Alberta for their efforts and cooperation.

6 REFERENCES

[1] CSA Z662-11; Oil and gas pipeline systems - Sixth Edition; Update No. 1: January 2012
[2] Wang, Ming L., Horsley D., Zhou J., 2006). “A quantitative approach to tensile strain capacity of pipelines” International pipeline conference, IPC2006-10474.
[3] Wang, Y.Y., Liu, M. and Horsley, D. (2007), "Strain based design of high strength pipelines " Proceedings of the 17th International Offshore and polar engineering conference (ISOPE 2007) Lisbon, Portugal, ISOPE, Vol 4, pp 3186-3193.
[4] Ostby, E. and Hellesvik, A. (2007), “Fracture control of offshore pipeline IP: results from large scale testing of the effects of biaxial loading on the strain capacity of pipes with defects” Proceedings of the 17th International Offshore and Polar Engineering Conference (ISOPE 2007), Lisbon, Portugal, July 1-6, Vol 4.
[5] Wang Y-Y.,et al (2011); “Second Generation Models for Strain-Based Design. Contract PR-ABD-1-Project 2. Final Approved Report Prepared for the Design, Materials and Construction Technical Committee of Pipeline Research Council International, (PRCI) Inc.
[6] Sandeep Kibey, et al "Tensile Strain Capacity Equations for Strain-Based Design of Welded Pipeline", ExxonMobil, IPC 2010-31661, pp.355-363.
[7] Fairchild, A.Kibey, et al, (2012). "Continued advancements regarding capacity prediction of strain-based pipelines", ExxonMobil, IPC 2012-90471, pp. 297-305
[8] Fairchild, et al "Advanced strain-based design pipeline welding technologies", ExxonMobil, IPC2014-33079.
[9] Meng Lin (2015) “Characterization of tensile and fracture properties of X52 steel pipes and their girth welds”, MSc Thesis, University of Alberta, Canada.
[10] Kibey, S, Issa, J, Wang, X, and Minnaar, K (2009). “A Simplified, Parametric Equation for Prediction of Tensile Strain Capacity of Welded Pipelines,” Presented at 5th Pipeline Tech Conference, Ostend, Belgium.